

Covalent organic frameworks as supports for a molecular Ni based ethylene oligomerization catalyst for the synthesis of long chain olefins

Rozhko, Elena; Bavykina, Anastasiya; Osadchii, Dmitrii; Makkee, Michiel; Gascon, Jorge

DOI

[10.1016/j.jcat.2016.11.030](https://doi.org/10.1016/j.jcat.2016.11.030)

Publication date

2017

Document Version

Accepted author manuscript

Published in

Journal of Catalysis

Citation (APA)

Rozhko, E., Bavykina, A., Osadchii, D., Makkee, M., & Gascon, J. (2017). Covalent organic frameworks as supports for a molecular Ni based ethylene oligomerization catalyst for the synthesis of long chain olefins. *Journal of Catalysis*, 345, 270-280. <https://doi.org/10.1016/j.jcat.2016.11.030>

Important note

To cite this publication, please use the final published version (if applicable). Please check the document version above.

Copyright

Other than for strictly personal use, it is not permitted to download, forward or distribute the text or part of it, without the consent of the author(s) and/or copyright holder(s), unless the work is under an open content license such as Creative Commons.

Takedown policy

Please contact us and provide details if you believe this document breaches copyrights. We will remove access to the work immediately and investigate your claim.

Covalent Organic Frameworks as Supports for a Molecular Ni based Ethylene

Oligomerization Catalyst for the synthesis of long chain olefins

Elena Rozhko, Anastasiya Bavykina, Dmitrii Osadchii, Michiel Makkee
and Jorge Gascon*

Delft University of Technology, Chemical Engineering Department, Catalysis
Engineering

Van der Maasweg 9, 2629 HZ Delft, The Netherlands

j.gascon@tudelft.nl

Abstract

The use of two different classes of covalent organic frameworks (covalent triazine and imine linked frameworks) as supports for molecular Ni²⁺ catalysts is presented. For COFs, a large concentration of N heteroatoms, either in the form of *quasi* bipyridine or as diiminopyridine moieties, allows for the coordination of NiBr₂ to the scaffold of the porous polymers. When applied as catalysts in the oligomerization of ethylene under mild reaction conditions (15 bar, 50 °C), these new catalysts display an activity comparable to that of their homogeneous counterpart and a five fold higher selectivity to C₆⁺ olefins. Accumulation of long chain hydrocarbons within the porosity of the COFs leads to reversible deactivation. Full activity and selectivity of the best catalysts can be recovered upon washing with dichlorobenzene.

Keywords: Ethylene oligomerization, Covalent Organic Framework, Ni catalyst, Porous Aromatic Polymers.

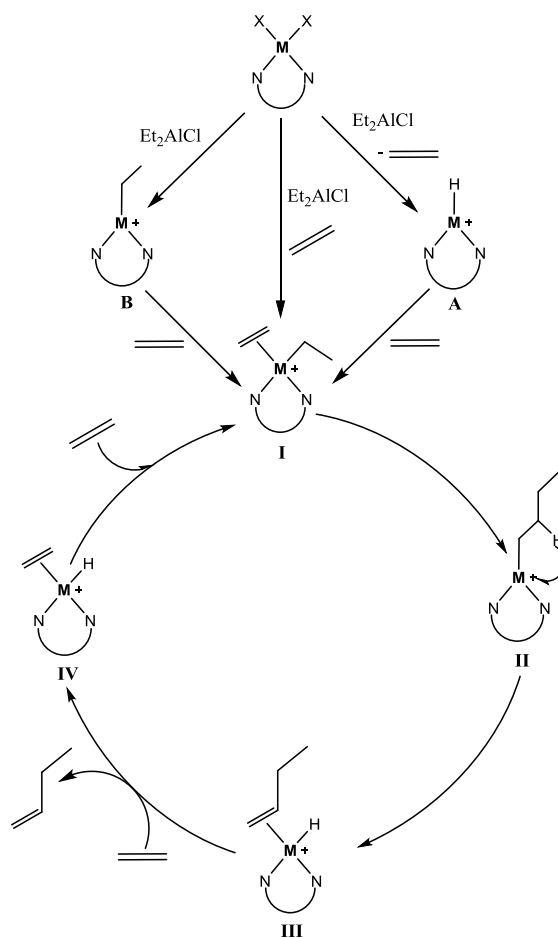
Introduction

α -Olefins in the C_4 – C_{20} range are of the utmost importance as they are valuable and versatile feedstocks and building blocks for a variety of products that people consume on a daily basis, i.e. detergents, plasticizers, polymers, etc. Currently oligomerization of ethylene is the prevalent method for the synthesis of these olefins [1].

Existing commercial processes utilise homogeneous catalysts. The two-step Ziegler stoichiometric process (INEOS), the one-step Ziegler process (Chevron-Phillips (CP) Chemicals) and the Shell higher olefins process (SHOP) are among the most widely applied industrial production methods together with the Idemitsu and SABIC processes. The two-step and the one-step Ziegler processes use triethylaluminum as a catalyst and SHOP is catalysed by nickel complexes, while Idemitsu and SABIC processes use a combination of Zr and alkylaluminium [2].

At the end of 1990s new efficient homogeneous catalysts were discovered and subsequently extensively studied. These are diimine and iminopyridine complexes of nickel, cobalt or iron in combination with alkylaluminum [3-14]. Though homogeneous catalysts in general show better performance, the use of a heterogeneous catalysts would be desired from a practical point of view, as it would ease catalyst handling and recycling and may result in enhanced selectivities to specially interesting products such as C_8 olefins. In this spirit, significant amount of research on heterogeneous catalysts has been performed in the past few decades. Among those, nickel-exchanged zeolites [15-24], Ni-MCM and Ni-SBA catalysts [25-33], supported $NiSO_4$ [34-41], supported NiO [42-48] and nickel-exchanged silica-alumina [49-53]. The most active Ni-exchanged zeolite [17] and silica-alumina catalysts [51] show the formation of mainly C_4 – C_8 olefins, with high selectivity to butenes (circa 70%). Selectivity to higher olefins can be enhanced by using bigger pore materials such as Ni-MCM catalysts [30, 32]. In all these cases, the formation of a minor amount of C_{10+} olefins was also detected (<10%). Supported $NiSO_4$ catalyses ethylene dimerization with selectivity to butenes of 100% [37, 39]. In case of supported NiO, at low temperatures (20°C) the only products are butenes, in contrast, when high temperatures (150-200°C) and high pressures are used, selectivity to butenes decreases to 10-13%, while, particularly, the formation of C_{6+} is enhanced.

From a design point of view, the immobilization of well optimized homogenous catalysts offers a number of advantages such as better selectivity control and metal utilization. This approach has been followed by several groups. In these works, diimine nickel complexes have been anchored to MCM-41 and MFS [54] and to hybrid silica [55], iminopyridine metal complexes have been supported on carbon nanotubes [56, 57] and diimine, iminopyridine, bis(imino)pyridine metal complexes have been immobilized into mica layered materials [58-62].



Scheme 1. Proposed mechanisms for ethylene oligomerization.

Catalysts supported on MCM-41, MFS and carbon nanotubes show a high activity in the polymerization of ethylene, while hybrid silica supported catalysts selectively form butenes of 100%. Another interesting and unique approach is reported by Malgas-Enus *et al.*, who used nickel metallodendrimers in a combination with alkylaluminum compound as catalyst, [63] reaching a maximum selectivity to butenes of 55%, with most of the other products being C₂₂-C₆₀ oligomers.

Recently, molecular heterogeneous catalysts based on Ni^{II} complexes supported on MOF materials were developed [64-69]. Another very interesting approach has been reported by Dinca's group by using a MOF support with a secondary building unit

structurally homologous to a 3-mesitylpyrazolyl Ni homogeneous catalysts [69]. In most cases, these catalysts display high selectivities to butenes (range from 85 to 95%) along with the formation of polyethylene on the surface of the catalyst [68].

The use of molecular catalysts requires the presence of a co-catalyst, alkylaluminum in most cases. According to the proposed reaction mechanisms [65, 68, 70, 71] (Scheme 1), reaction with alkylaluminum has been proposed to either promote proton abstraction to active metal-hydride species (A), or to generate mono (B) or dialkylated (I) metal adducts. In case of metal-hydride or monoalkylated metal species, the next step is the insertion of ethylene to form a dialkylated adduct (I). Then the formation of an alkyl-metal intermediate (II) takes place that leads to intermediate IV after releasing butene through β -hydride elimination. Further inclusion of additional ethylene molecules on complex (II) yields to the formation of higher olefins that are finally released via β -hydride elimination

When looking at the reaction mechanism and at the examples summarized above, it is clear that prediction of the product spectrum of a given catalyst is not trivial, although, in general, it is proposed that stabilization of the first oligomerization product (III) at the surface of the catalyst is crucial in determining the “chain growth probability” of the process. In this line, hydrophobic supports seem to result in the production of a larger amount of longer olefins, while more hydrophilic supports mostly produce butenes.

In light of the existing literature, we decided to explore the use of Covalent Organic Frameworks (COFs), more specifically, of Porous Aromatic Frameworks (PAFs), as potential supports for Ni ethylene oligomerization catalysts. PAFs consist only of light elements (C, N and H) and display a high degree of tunability, both in terms of pore size and surface area. In this spirit, we studied the use of two different families of PAFs: Covalent Triazine Frameworks (CTFs) with micro- and mesoporous structures, and a lamellar structured imine-linked polymer network (IL-PON). In both cases, a large concentration of N heteroatoms (either in the form of *quasi* bipyridine moieties in case of CTFs or in the form of diiminopyridine moieties in case of the IL-PON) within the porous structure of these materials allows for the direct coordination of Ni^{2+} . Our results demonstrate that both families of solids hold great promise for the selective formation of C_8 olefins and that deactivation of the catalysts due to the adsorption of C_8 - C_{30} products can be easily mitigated by catalyst reactivation in dichlorobenzene.

Experimental section

Materials

1,3,5-Tris(*4*-aminophenyl)benzene was purchased from TCI Europe N.V. and used as received. All other reagents and solvents were purchased from Sigma-Aldrich and used as received.

Catalysts synthesis

Synthesis of imine-linked porous organic network (IL-PON)

The following general procedure was followed to prepare the *IL-PON* support: 116 mg (0.858 mmol) of 2,6-pyridinedicarboxaldehyde were dissolved in 10 ml of DMSO; 200 mg (0.569 mmol) of *1,3,5*-tris(*4*-aminophenyl)benzene were dissolved in another 10 mL of DMSO. Then, solutions were mixed in a round-bottom flask and 1 mL of 99.8% acetic acid was added. Almost immediately there was a formation of the yellow polymer. Polymer was subsequently washed with methanol and THF and dried at 150°C under vacuum giving 286 mg (yield based on the monomers ~90%) of a yellow powder.

Synthesis of mesoporous and microporous Covalent Triazine Framework (meso-CTF and micro-CTF)

To synthesise microCTF, a glass ampoule was charged with with 2,6-pyridinedicarbonitrile (0.124 g, 0.96 mmol) and anhydrous ZnCl₂ (0.664 g, 4.8 mmol) in a glovebox. For the mesoCTF, the ampoule was charged with 2,6-pyridinedicarbonitrile (0.041 g, 320 μmol), 4,4'-biphenyldicarbonitrile (0.131 g, 640 μmol) and anhydrous ZnCl₂ (0.664 g, 4.8 mmol). The ampoule was flame sealed and the mixture was heated at 500°C for 48 h and then cooled to room temperature. The product was consecutively washed in 5M HCl at 100°C, in NH₄OH at 60°C, in H₂O at 100°C and then in THF at 60°C, each step overnight. The washing steps might seem excessive, but were, as we found, required to remove ZnCl₂. Finally, the powder was dried in vacuum at 180°C overnight.

*Coordination of DME*NiBr₂*

A mixture of 0.1 g of Nickel(II) bromide ethylene glycol dimethyl ether (DME*NiBr₂) and 15 mL of THF was placed in a round-bottom flask and stirred for 5 minutes, then 0.2 g of a polymer was added. The mixture was stirred at 67°C overnight and filtered. Afterwards, the powder was washed with 50 mL of fresh THF at 70°C overnight to remove DME. The final product was filtered and dried under vacuum at 100°C.

Characterization Techniques

Argon adsorption was performed on a Micromeritics ASAP 2010 gas adsorption analyser (stainless steel version) at -186 °C. For the DFT calculations on the pore size distribution, the MicroActive v. 3.00 (Micromeritics) software package was used using a Argon on oxides at 87K NLDFT (Non Local Density Functional Theory) model for CTF based samples, using a non-negative regularization method with a factor of 0.03160, Standard Deviation of Fit: 0.99706 cm³/g STP for micro-CTF, 0.55780 cm³/g STP for Ni@micro-CTF, 0.85175 cm³/g STP for meso-CTF and 0.58938 cm³/g STP for Ni@meso-CTF. Carbon slit pores NLDFT model was used for IL-PON based samples, using a non-negative regularization method with a factor of 0.20000, Standard Deviation of Fit: 3.35521 cm³/g STP for IL-PON, 1.23988 cm³/g STP for Ni@IL-PON. XPS measurements were performed on a *K-alpha* Thermo Fisher Scientific spectrometer using a monochromatic Al *Kα* X-ray source. The measurements were performed at ambient temperature and chamber pressure of about 10⁻⁷ mbar. A flood gun was used for charge compensation. All the spectra measured were corrected by setting the reference binding energy of carbon (C1s) at 285.0 ± 0.025 eV. Spectra were analysed using the Thermo Avantage software package, background subtraction is done using the setting “SMART”. From the intensity ratios, the following selectivity factors were used – 3.726 for Zn, 4.044 for Ni and 0.477 for N.

For elemental analysis, the Ni@CTF samples were analyzed by Mikroanalytisches Laboratorium KOLBE, (Mülheim an der Ruhr, Germany), Ni@IL-PON samples were analyzed using PerkinElmer Optima 5300 (torch:4300) instrument, with ICP-OES 5300DV. CHN analysis was also performed by Mikroanalytisches Laboratorium KOLBE, (Mülheim an der Ruhr, Germany) using a CHN-Analyser from Elementar Model Vario EL.

Scanning electron microscopy (SEM) images were recorded using a JEOL JSM-6010LA with a standard beam potential of 10 kV and an Everhart-Thornley detector. X-ray microanalysis (SEM/EDX) confirmed the elemental composition in the sample by the scanning electron microscopy (SEM) coupled with a dispersive X-ray microanalysis system (EDX) with a Silicon-drift detector.

Diffuse reflectance infrared Fourier transform spectroscopy (DRIFTS) was performed in a Bruker model IFS66 spectrometer equipped with a high temperature cell with CaF₂ windows and a 633 nm laser. The spectra were registered after accumulation of 128 scans and a resolution of 4 cm⁻¹. A flow of helium at 10 ml/min was maintained during the measurements. Before collecting the spectra, the different samples were pre-treated in a helium flow at 393 K for 30 min. KBr was used for background.

Thermogravimetric analysis (TGA) was performed on a Mettler Toledo TGA/SDTA851e equipment, where 0.011–0.02 g of samples was screened for the change in its mass while heated from 303 to 1273 K with a heating rate of 2 K min⁻¹ under air flow.

The gas phase was analyzed by a CompactGC4.0 from Interscience equipped with a FID detector and two consecutive columns: Rt-QBond, length 14 m, diameter 0.32 mm, and Rt-UBond, length 10 m, diameter 0.32 mm. Liquid phase was analysed by GC (Agilent 7890A) equipped with a FID detector and Durabond (DB-1) column, length 30 m, diameter 0.25 mm.

Transmission Electron Microscopy (TEM) analysis was performed in a JEOL JEM-1400-Plus microscope operated at 120 keV with LaB6 emission filament.

Ethylene oligomerization

Oligomerization experiments were performed in a Parr 5000 Multi Reactor Stirrer System under ethylene pressure (batch conditions). The reaction vessels (autoclaves) have a volume of 45 mL and were stirred at 1000 rpm with suspended magnetic bars. Autoclaves were filled inside the glovebox with 20 mL of heptane as solvent, 1.2 mL of the 1M triethylaluminum solution in heptane as a co-catalyst and 20 mg of Ni@micro-CTF, Ni@meso-CTF or Ni@IL-PON as catalyst. Before starting the reaction the air in lines was removed by consecutive pressurizing and depressurizing the system with He. Ethylene was then introduced in the autoclaves until a pressure of 15 bar was reached. The autoclaves were heated to the desired temperature with a heating rate of 2 °C min⁻¹ and kept at this temperature for 2 hours. After the reaction, the gas mixture was collected with gas-bags and the liquid-phase was separated from the catalyst.

In every case, the spent catalyst was filtered from the reaction mixture using a Nylon filter with 0.45µm pore size, washed in heptane at 50 °C for 1 hour and dried overnight. Afterwards, fresh heptane and triethylaluminum were added to the catalyst and reaction repeated as described above.

A series of blank experiments were also carried out: (1) in the presence of only activator Et₃Al; (2) in the presence of only catalyst; (3) only heptane, to estimate ethylene solubility under chosen conditions. From the blank experiment (3), the dimensionless Henry solubility was calculated:

$$H^{cc} = \frac{C_a}{C_g}, \text{ where } C_a \text{ is liquid-phase concentration and } C_g \text{ is gas-phase concentration, At}$$

20°C and 15 bar of initial pressure, a value of 0.66 was found for H^{cc} .

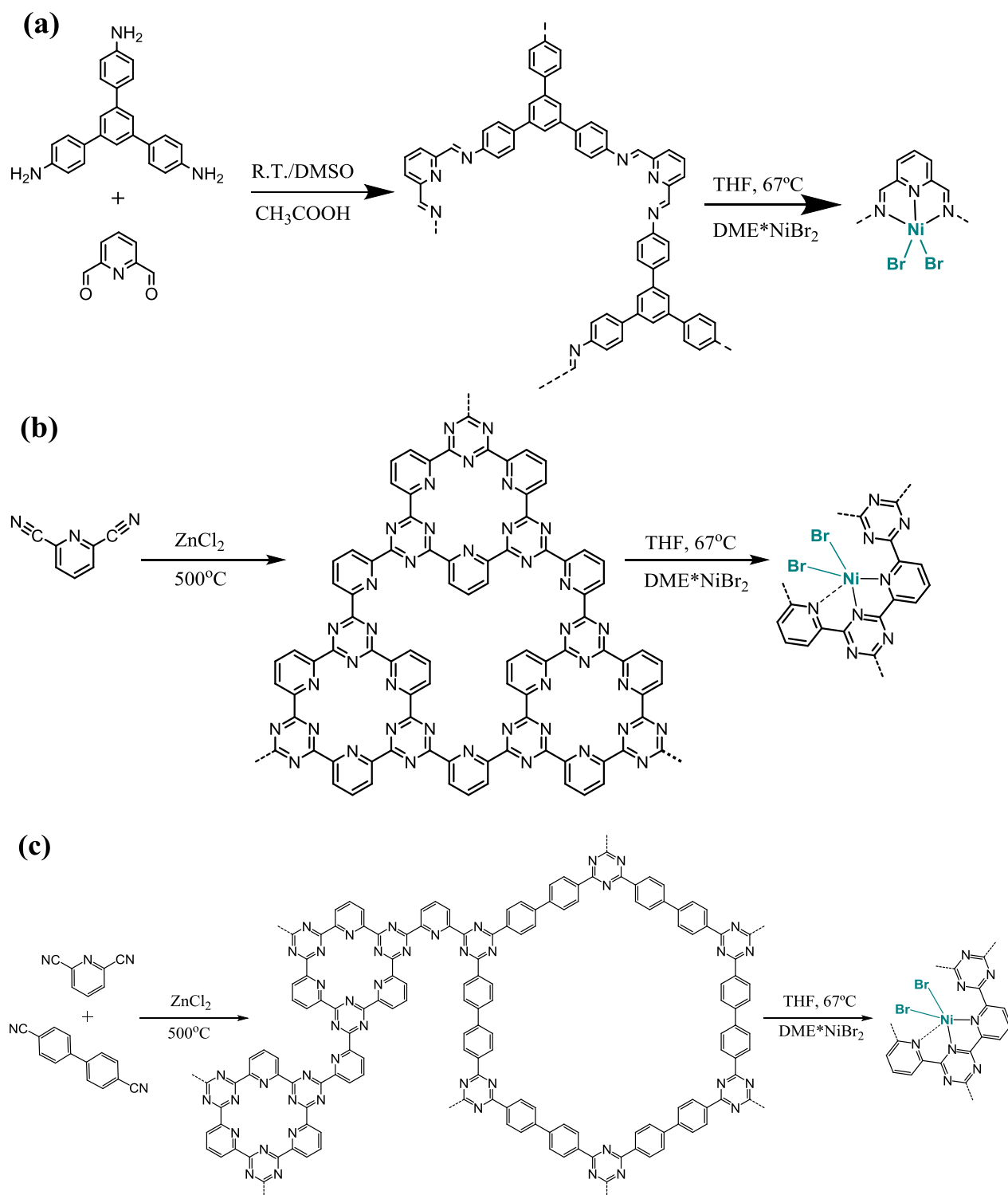
Selectivity (*S*) and total number of turnovers (*TON*) were calculated according to the following equations:

$$S = \frac{n_{\text{product}}(\text{mol})}{\Sigma n_{\text{product}}(\text{mol})} \cdot 100\%$$

$$TON = \frac{n_{\text{converted carbon}}(\text{mol})}{n_{\text{Ni}}(\text{mol})}$$

Results and Discussion

With the aim of exploring the suitability of different highly stable PAFs as supports for the immobilization of Ni, we selected two different types of solids: type one, the so called IL-PON is an diiminopyridine PAF and was synthesized via the acid catalysed condensation of 2,6-pyridinedicarboxaldehyde and 1,3,5-tris(4-aminophenyl)benzene, as previously described by Zamora *et al.* [72] (scheme 2a).



Scheme 2. Synthesis of the IL-PON through polyimine condensation (a), micro-CTF (b) and meso-CTF (c) and expected coordination of Ni²⁺ to the nitrogen species in the frameworks.

The second type of supports belongs to the family of Covalent Triazine Frameworks (CTF, see scheme 2b,c), a highly porous class of organic polymers synthesized through the high temperature polymerisation of nitrile containing aromatic building blocks. In

order to tune the final porosity of the CTF, we synthesized a purely microporous material based on the polymerisation of 2,6-pyridinedicarbonitrile (denoted as micro-CTF) and a micro-mesoporous solid obtained from the condensation of 2,6-pyridinedicarbonitrile and 4,4'-biphenyldicarbonitrile in a 1:2 ratio (denoted as meso-CTF). Synthesis methods previously reported by our group were followed for the preparation of the CTF supports [73].

The successful imine condensation during the synthesis of IL-PON was confirmed by diffuse reflectance infrared Fourier transform (DRIFT) spectroscopy (Figure 1a). DRIFT spectrum of the polymer shows the presence of C=N (1597 cm^{-1}) and C-C=N-C (1287 cm^{-1}) moieties, while the C-N stretching mode from the 1,3,5-tris(4-aminophenyl)benzene precursor (1279 cm^{-1}) is not present in the final solid, demonstrating the full polymerization of the monomers [72, 74].

The Argon adsorption isotherm of IL-PON (Figure 1b) displays the typical "house of cards" shape with a low pore volume accompanied by a relatively larger uptake at moderate pressures. We attribute the three different regimes in the isotherm to adsorption in the pore mouth of the lamellar material ($P/P_0 < 0.05$), formation of several Ar layers on the surface of the lamellas ($0.05 < P/P_0 < 0.7$) and condensation of Ar in the interlamellar space ($0.7 < P/P_0 < 0.98$). [75]

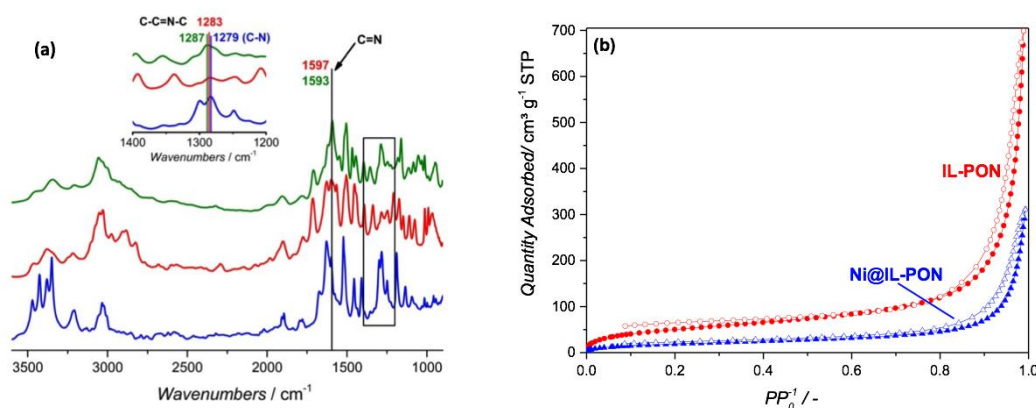


Figure 1. (a) DRIFT spectrum of 1,3,5-tris(4-aminophenyl)benzene (blue), IL-PON (red) and Ni@IL-PON (green); (b) Argon adsorption isotherms at -186 °C for IL-PON support (red) and Ni@IL-PON catalyst (blue). Close symbols correspond to the adsorption and open symbols to desorption branches.

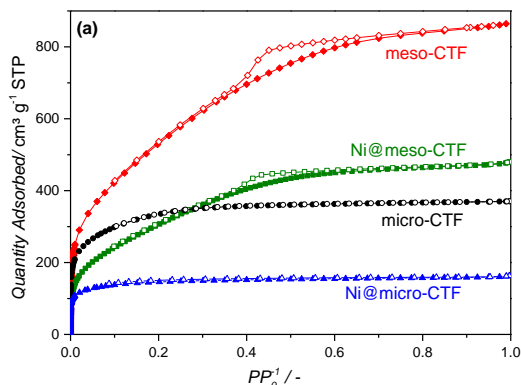


Figure 2. Argon adsorption isotherms at -186 °C for micro-CTF support (black), Ni@micro-CTF catalyst (blue), meso-CTF support (red) and Ni@meso-CTF catalyst (green). Close symbols correspond to the adsorption and open symbols to desorption branches.

In contrast, adsorption isotherms on both CTF materials (Figure 2) show the fully microporous nature of micro-CTF and the micro-meso porous character of meso-CTF, in good agreement with our previous results [73, 76]. Table 1 summarizes the main textural properties of the different supports and catalysts.

Table 1. Textural properties of polymers and catalysts

Sample name	BET surface area / m^2g^{-1}	Pore volume / cm^3g^{-1}
IL-PON	106	0.87
Ni@IL-PON	86	0.34
meso-CTF	1803	1.15
Ni@meso-CTF	1439	0.63
micro-CTF	930	0.54
Ni@micro-CTF	330	0.24

CHN analysis performed on the three different supports revealed the following C:H:N ratios: IL-PON: 82.3: 5.5: 12.2; micro-CTF: 69.7: 3.0: 27.3; meso-CTF: 87.1: 2.0: 10.9. When compared to the expected values according to polymerization stoichiometry (81.2:3.9:14.9; 65.1: 2.3: 32.6; and 78.2: 3.5: 18.2), the obtained N content is circa a 80% of the expected one for IL-PON and micro-CTF and 60% of the expected ratio for meso-CTF. While in case of IL-PON and micro-CTF this can be attributed to the

presence of solvent occluded in the pores and/or to the high temperature used for the formation of the CTF (see XPS characterization, *vide infra*), in case of meso-CTF, this may be an indication of a slightly different polymerization ratio between the two monomers used.

Ni²⁺ was coordinated to the diiminopyridine and *quasi* bipyridine moieties of the support materials by excess impregnation of Nickel(II) bromide ethylene glycol dimethyl ether (DME*NiBr₂) under mild conditions. Upon a one-step impregnation, Ni loadings of 4.7, 2.8 and 2.8 wt % were obtained for Ni@IL-PON, Ni@micro-CTF and Ni@meso-CTF, respectively. These loadings correspond to molar N:Ni ratios of 10, 40 and 16, respectively and demonstrate that in all cases not all potential coordination sites are occupied by Ni.

TEM micrographs of the different catalysts (see supplementary information file) reveal the expected lamellar structure of IL-PON and a good dispersion of Ni (note that no metal nanoparticles could be observed in any of the samples). On the other hand, the three polymers seem to macroscopically result from the agglomeration of small (10-50 nm) primary particles.

Thermogravimetric analysis (TGA) under air atmosphere (see figure 8) shows that all catalysts are stable up to 400°C under oxidizing conditions, with all samples presenting only a small weight loss under 100°C attributed to the loss of remaining solvent and moisture. The presence of Zn from the synthesis of meso-CTF is clear from the larger residue found on the TGA analysis of the fresh catalyst and from the XPS analysis below.

Coordination of Ni²⁺ leads to a decrease in surface area for all catalysts (see figures 1 and 2 and table 1), with a much bigger impact on micro-CTF, where a 65% of the

available porosity is lost after incorporation of a 2.8 wt% of Ni. In contrast, only a loss of a 20 % is observed for the bigger pore CTF material upon introduction of a similar amount of Ni and for the IL-PON upon coordination of a 4.7 wt% of Ni. These results are in good agreement with the expected accessibility of each support: in case of micro-CTF, addition of the relatively bulky NiBr₂ moieties would produce the blockage of part of the porosity, while addition of mesopores already mitigates this effect in meso-CTF. On the other hand, with most surface being available as external surface for the IL-PON, the effect on final textural properties is even smaller. The available external surface together with the fact that all N atoms from the framework can engage in coordination explain the higher metal loading achieved for IL-PON.

In order to study the coordination of Ni²⁺ to the frameworks, X-ray photoelectron spectroscopy (XPS) (Figures 3-5) was performed before and after Ni²⁺ impregnation. Table 2 shows the relative surface content of N, Zn and Ni for all samples. One can see that the Ni:N ratio on the surface is much higher for Ni@micro-CTF compared to Ni@IL-PON and Ni@meso-CTF. It indicates that micro-CTF is less accessible for Ni compared to IL-PON and meso-CTF, in good agreement with the data from adsorption measurements. XPS shows the presence of residual Zn on the surface of CTF samples, coming from ZnCl₂ used as catalyst for CTF synthesis. Introduction of Ni leads to further decrease of Zn surface content, and its amount can be considered insignificant compared to the surface content of Ni after coordination.

Table 2. Relative content of Ni and Zn in different catalysts

Sample	I_{Zn2p}/I_{N1s}	I_{Ni2p}/I_{N1s}
Ni@IL-PON	-	0.31
micro-CTF	0.06	-
Ni@micro-CTF	0.06	0.54
meso-CTF	0.15	-

According to the synthesis procedure, Ni can be either chemically coordinated to N functional sites of the framework or remain on the surface and in the pores as non-coordinated complexes or clusters. In order to reveal the chemical state of Ni in the catalysts, high resolution spectra of N1s and Ni2p line were analysed. Fig. 3 shows Ni2p spectra for all samples after Ni introduction. All spectra represent the line shape typical for Ni²⁺ compounds, however, binding energies of the main Ni2p_{3/2} peak are different: 855.3 eV for Ni@IL-PON and 856.1 eV for Ni@CTF samples. These binding energies definitely do not correspond to Ni(II) oxide NiO (main peak at 853.7 eV), but are in the range of typical values for most of Ni-O and Ni-N complexes [77].

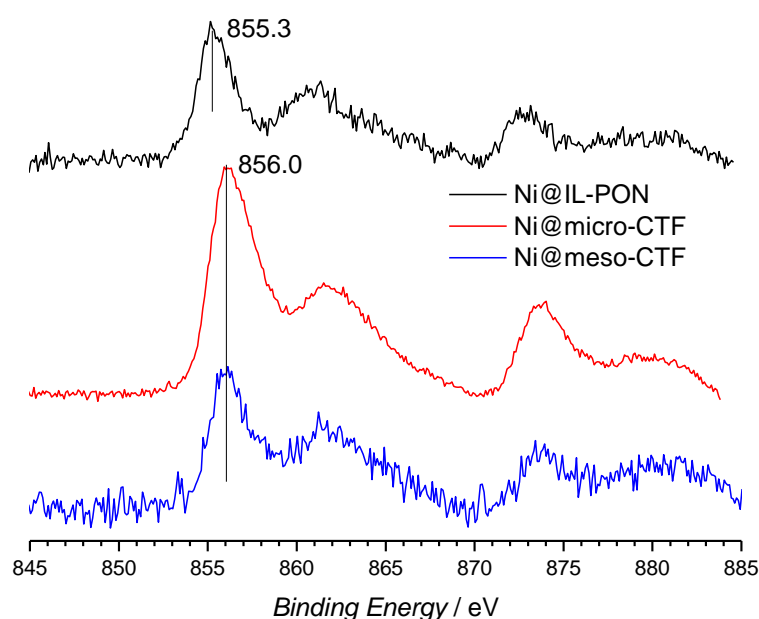


Figure 3. Ni2p XPS spectra of Ni@IL-PON, Ni@micro-CTF and Ni@meso-CTF catalysts.

Fig. 4 shows N1s line of IL-PON before and after introduction of Ni. The main peak of N1s line with binding energy of about 398.6 eV is clearly shifted to a higher binding energy (399.3 eV), indicating the donation of electron density from N atoms, something normally observed upon coordination of N-containing groups to metal ions [78]. Additional peaks of N1s line of

IL-PON with higher binding energy (400.1 eV, 401.8 eV) disappear after Ni coordination, that let us attribute it to unreacted monomer and other non-framework species removed during the process of Ni introduction and washing.

A similar, but less pronounced, behaviour is observed in case of micro-CTF and meso-CTF species. N1s lines of CTF samples consist of three peaks. First peak with binding energy of 398.2 eV in case of meso-CTF and 398.4 eV in case of micro-CTF corresponds to pyridinic N species of the framework. Peaks at higher binding energy (399.8 and 401 eV), corresponding to partial framework decomposition due to high temperature treatment (pyrrolic and quaternary N species, respectively) [78, 79]. Introduction of Ni shifts the first peak to higher binding energy: this shift is very small in case of micro-CTF (0.2 eV) and more obvious in case of meso-CTF (0.4 eV). For both samples the binding energy of pyridinic N1s peak becomes equal to 398.6 eV after coordination of Ni. No shift is observed for peaks with binding energy of 399.8 and 401 eV, indicating preferential coordination of Ni to pyridinic N species within the CTF. However, the observed shifts are small compared to the one observed in case of IL-PON samples. This might indicate weaker coordination of the Ni²⁺ ions in case of the CTF materials.

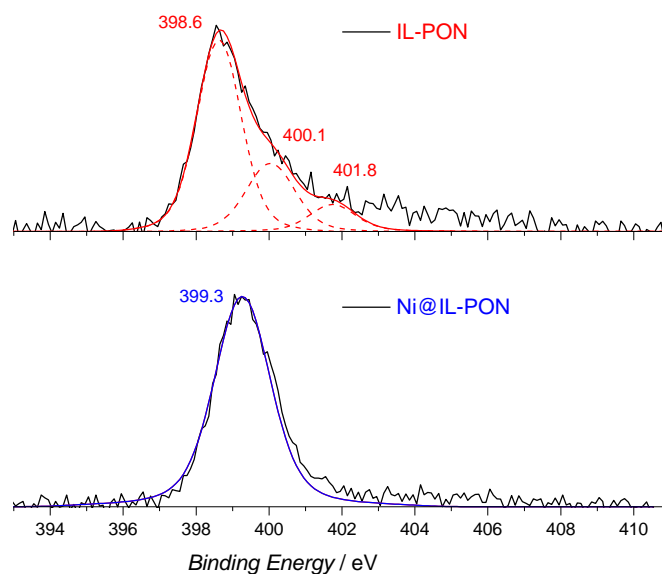


Figure 4. N1s XPS spectra of pristine IL-PON polymer and Ni@IL-PON catalyst.

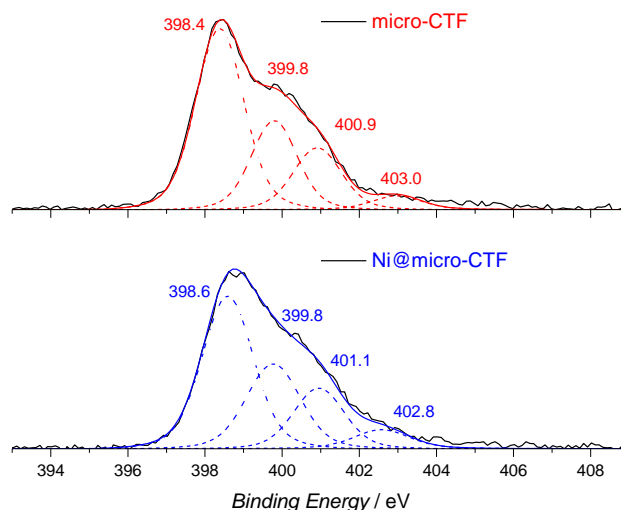


Figure 5. Ni 1s XPS spectra of pristine micro-CTF and Ni@micro-CTF catalyst.

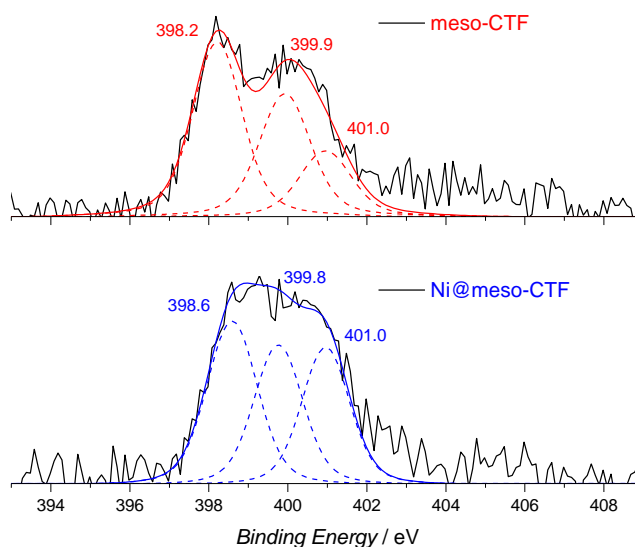


Figure 6. Ni 1s XPS spectra of pristine meso-CTF and Ni@meso-CTF catalyst.

A possible explanation for this effect could be attributed to the difference between N-containing coordination sites of CTFs and IL-PON. IL-PON contains pincer-like diimino-pyridinic groups in its structure that afford strong coordination of metal ions with its three nitrogen atoms. CTFs contain 6-membered triazino-pyridinic rings with 6 nitrogen atoms inside the ring (see figure 2), but size of the ring will be too large for Ni²⁺ ion in this case, so it would probably be coordinated only to two nitrogen atoms of six, leading to a weaker complex.

The catalytic performance in ethylene oligomerization of the different PAF based catalysts was studied in batch mode at 50°C under initial ethylene pressure of 15 bar in heptane using 20 mg of catalyst and Et₃Al as co-catalyst. When the pressure in the reactor reached 15 bar, reactors were switched to a batch mode and stirring of the mixtures started. Due to the stirring, part of ethylene dissolves in heptane and pressure drops to about 8 bar. Reactor loading and all manipulations with reaction mixtures were carried out under inert atmosphere to avoid decomposition of Et₃Al.

Table 2 shows the total number of turnovers achieved by each catalyst based on the analyzed amount of liquid and gaseous products along with the selectivity to C₄, C₆ and C₆₊ olefins. While blank experiments performed with only Et₃Al or PAF catalyst did not result in any conversion of ethylene, the combination of the solid catalyst and the homogenous co-catalyst was active. The obtained total number of turnovers is lower than reported for the homogeneous counterpart ((bpy)NiBr₂) under similar reaction conditions and time on stream [68], but for every PAF based catalyst at 50 °C, the selectivity to higher olefins is 5 times larger than that of the homogeneous one and 3 times bigger for experiments performed with the Ni@IL-PON catalyst at room temperature.

Table 3. Ethylene oligomerization catalysed by Ni containing catalysts.^a

Entry	Catalyst	Selectivity, %				TON ^{b,c}
		C ₄₌	C ₆₌	C ₈₌	C ₁₀₊	
0[68]	(bpy)NiBr ₂ (2.8 μmol)	90	10	0	2240±100	
1	Ni@IL-PON (16 μmol)	58	20	15	7	370±60
2	Ni@micro-CTF (9.6 μmol)	59	9	29	3	252±6
3	Ni@meso-CTF (9.6 μmol)	54	17	17	12	301±50
4	Ni@meso-CTF (9.6 μmol) ^d	68	15	10	7	269
5	Ni@IL-PON-RT (16 μmol) ^e	70	14	10	6	561±30

[a] Reaction were carried out in a batch mode at 50°C, with 15 bar of initial pressure of ethylene, heptane as a solvent, 20 mg of catalyst, 1.2 mmol of Et₃Al as an activator. [b] TON were calculated as the moles of carbon converted/moles of Ni, after 2 hours of reaction. The amounts of products formed were calculated from GC-FID analysis of the reaction mixture. This number does not include the possible formation of alkenes bigger than C₂₀. [c]

The value is given as average of two experiments. [d] 0.7 mmol of Et₃Al (Al/Ni = 70), one run. [e] Experiments were performed at 25°C.

Although small increases (i.e. 5 or 10 points) in selectivity to higher olefins have been reported upon immobilization of similar homogeneous systems [80], the ones found here are remarkable. When comparing the COF based catalysts with each other, in spite of the small differences found in number of turnovers, these results are in good agreement with the textural properties of the solids: on one hand, Ni@IL-PON, in spite of containing the highest amount of Ni, displays the highest activity per atom of metal, followed by the mesoporous material and with Ni@micro-CTF being the least active. These results suggest a link between active site accessibility and catalytic performance, with the small pore material most likely suffering from internal diffusion limitations and from the fact that not all Ni has been coordinated to the N moieties (*vide supra*). On the other hand, clear differences are found in terms of selectivities: while Ni@IL-PON displays a product distribution close to a classical ASF polymerization, with selectivity decreasing with the number of carbons in the olefin, the Ni@micro-CTF sample shows higher selectivities to C₈₌ than to C₆₌. A similar trend, although less prominent, is found for Ni@meso-CTF. We rationalize these results on the basis of re-adsorption of products due to a slower diffusion in the micropores of both CTFs, leading to further oligomerizations. In this way, C₄₌ formed in the external surface of the particles would directly desorb, while those olefins forming inside the narrow micropores will suffer subsequent reactions leading to higher hydrocarbons. This effect is less important in case of the micro-meso catalysts, where diffusion of products will be faster than in case of micro-CTF.

Table 4. Comparison of reported catalytic activity of heterogeneous catalysts for ethylene oligomerization.

Entry	Catalyst	T, °C	P, bar	Al/Ni	Ni, wt%	S _{C₄} , %	S _{C₆₊} , %	Reference
1	Ni@IL-PON	50	15	70	4.7	58	42	This study
2	Ni@micro-CTF	50	15	100	2.84	59	41	This study

3	Ni@meso-CTF	50	15	100	2.83	54	46	This study
4	Ni@meso-CTF	50	15	70	2.83	68	32	This study
5	Ni@IL-PON-RT	25	15	100	4.7	70	30	This study
6	Ni@MIL101	25	30	70	2	95	5	[65]
7	Ni@MOF	5	15	70	27.7	89.1	10.9	[64]
8	NU-1000-bpy-NiCl ₂ ^a	21	15	70	2.7	93	7	[68]
9	Ni@MixMOF	40	20	100	1.17	92.7	7.3	[66]
11	Ni-MFU	50	15	100	10	85.2	14.8	[69]
12	Ni(N,N)/MCM-41	25	12	5	3.5	84	5.8	[81]
13	Ni(P,P)@silica	60	10	250	n.a.	54	45	[82]

^a Pressure was kept constant at 15 bar during the reaction.

When compared to the literature (see table 4 and references [64-68, 81, 82]), the selectivity of the PAF based catalysts to medium chain olefins is higher than those reported for other systems based either on MOFs or silica based supports. With this comparison, one should keep in mind that experiments here reported were performed at slightly higher temperatures (50 vs. 20-25 °C) than in most of the references listed in table 3. We intentionally chose a slightly higher temperature than that commonly used in order to have a better control over reaction conditions.

It is indeed well known that the rate of the β -H elimination displays the lowest activation energy and may become the rate limiting step at higher temperatures (see Figure 6.1), leading to higher selectivities to C₆₊ olefins and to lower overall reaction rates. [83] However, even for those cases where similar reaction temperatures were used (table 4 entries 9, 11 and 13) the selectivity shown by the PAF based catalysts to longer hydrocarbons is striking. In the same line, experiments performed with the Ni@IL-PON at room temperature (table 4, entry 5) display at least a three-fold increase in selectivity to C₆₊ compared to other systems. Only in case of the wide pore silica Ni phosphine immobilized catalyst in entry 13, similarly low selectivities to C₄₌ have been reported,

even when these expensive P containing ligands are known to promote the formation of longer hydrocarbons [80].

The results presented so far demonstrate that the chosen PAFs display catalytic performances in terms of activity not far from their homogenous counterparts and selectivities to more interesting olefins (C_{8+}) higher than for most homo and heterogeneous catalysts reported to date based on Ni-pyridine systems. We attribute this change in selectivity to the higher affinity of the fully organic PAF supports for the reaction products, that may lead to a higher surface concentration of olefins and therefore to higher chances for multiple oligomerization reactions.

In order to further explore the catalytic stability of these new systems, we studied their re-use in consecutive catalytic runs. Recyclability experiments were performed after recovering the used catalyst *via* filtration and washing in heptane at 50°C for 1 hour followed by overnight drying.

Figure 7 shows the changes observed in activity and selectivity over 5 consecutive runs for all catalysts, while detailed changes in selectivity after each run are given in the supplementary information file.

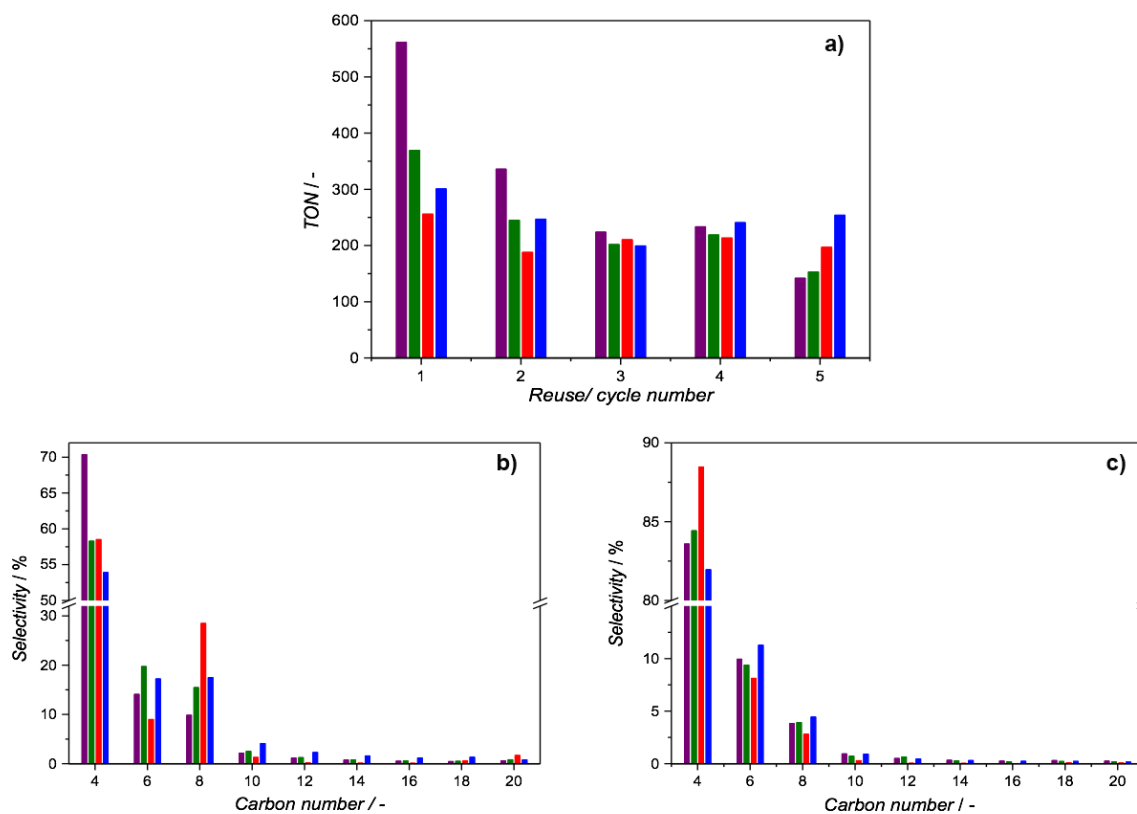


Figure 7. (a) Catalytic activity in ethylene oligomerization reaction vs. number of cycles and change of selectivity vs. cycle for Ni@IL-PON (experiments performed at room temperature) (purple), Ni@IL-PON at (green), Ni@micro-CTF (red) and Ni@meso-CTF (blue): (b) 1st cycle, (c) 5th cycle. Reaction conditions: 20 mL of heptane as solvent, 1.2 mL of 1M triethylaluminum solution in heptane as a co-catalyst and 20 mg of catalyst. T = 50 °C; reaction time = 2 h; P_0 =15 bar; autoclave volume = 45 mL.

Going from the first to fifth cycle selectivity to butenes rises up and reaches values over 80%, while the formation of $C_{8=+}$ oligomers becomes negligible for all samples. Surprisingly, both in terms of activity and selectivity, the microporous CTF catalyst is the one that suffers the smallest decline. A decrease in selectivity to longer hydrocarbons along with a clear drop in catalytic activity after the first reaction cycle can be rationalized on the basis of pore blocking by either the co-catalyst or by the retention of ethylene oligomers within the porosity of the material. In order to quantify the effect of both processes, we performed a thermogravimetric analysis of the spent catalysts after one reaction cycle. TGA analysis of spent catalysts (Figure 8) confirms the presence of an additional inorganic residue (attributed to a mixture of Al_2O_3 and

NiO upon calcination) and the presence of carbon deposits that are combusted at circa 300 °C, prior to the decomposition of the organic frameworks, pointing to the presence additional olefins adsorbed within the porous scaffolds.

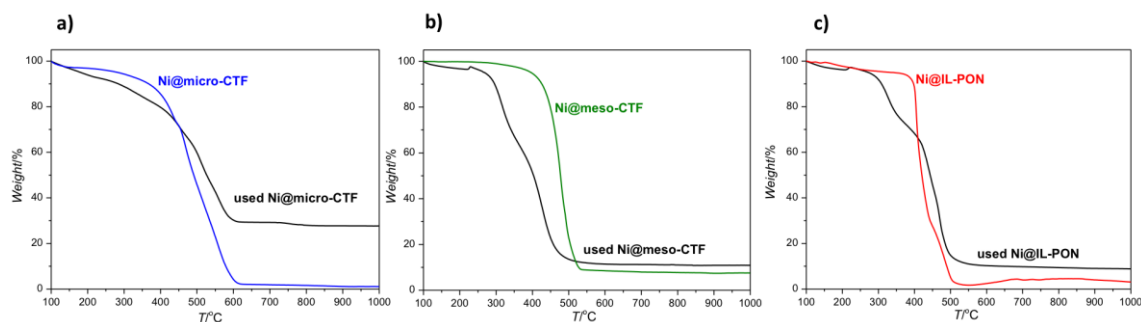


Figure 8. TGA analysis in air of fresh and spent catalysts after one reaction cycle. Heating rate = 2 °C min⁻¹

From figure 8, it is clear that the mesoporous CTF and IL-PON contain a bigger amount of adsorbed olefins. Hence, the lower decrease in activity and selectivity of the micro-CTF can be explained by the lower formation of long hydrocarbons within the porosity of the material, most likely due to the fact that most reaction takes place at the surface of the catalyst's particles. On the other hand, although Ni@meso-CTF seems to accumulate a minor amount of Al species, no clear correlation between this accumulation and the observed deactivation can be drawn at this point.

With the aim of fully recycling these catalysts and having in mind that the observed deactivation is mostly due to the formation of long chain olefins non soluble in heptane, we performed additional experiments by recycling the catalysts with an intermediate washing step using dichlorobenzene instead of heptane. The choice of the solvent was based on the much higher solubility of long chain olefins on the aromatic solvent. When using this procedure (Figure 9), both mesoporous PAF based catalysts (IL-PON and meso-CTF) fully recover their initial activity, while the smaller pore Ni@micro-CTF still presents a drop in activity similar to that shown after washing with heptane. On the other hand, Ni@IL-PON and Ni@micro-CTF display a slightly higher selectivity to C₄

olefins while Ni@meso-CTF exhibits a similar product distribution as during the first cycle. GC analysis of the 1,2-dichlorobenzene used in the washing step demonstrated the presence of olefins up to C₃₀ for all three catalysts. These results demonstrate that the main reason for deactivation is strong adsorption of long chain olefins within the porosity of the different catalysts, but also infers that adsorption of the Al activator may play a role in the observed lower selectivities of Ni@IL-PON and Ni@micro-CTF after recycling. Current efforts are focused on the inclusion of an activator function within these scaffolds with the objective of developing a truly heterogeneous catalyst that does not require the use of alkylaluminum in solution.

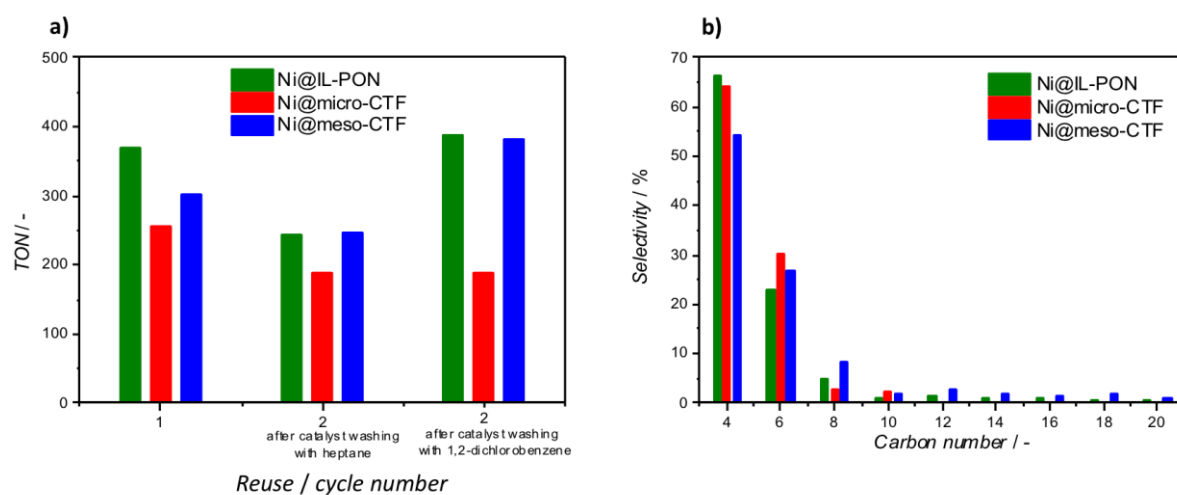


Figure 9. a) Effect of catalyst reactivation conditions on catalytic activity expressed as number of turnovers (TON) after 2 hours of reaction. b) Olefin selectivity after catalyst re-activation with 1,2-dichlorobenzene. Reaction conditions: 20 mL of heptane as solvent, 1.2 mL of 1M triethylaluminum solution in heptane as a co-catalyst and 20 mg of catalyst. T = 50 °C; reaction time = 2 h; P₀=15 bar; autoclave volume = 45 mL.

Conclusions

In summary, we have explored the use of two different classes of covalent organic frameworks (covalent triazine and imine linked frameworks) as supports for molecular Ni²⁺ catalysts. A thorough XPS analysis of these materials demonstrates that the large concentration of N heteroatoms, either in the form of *quasi* bipyridine moieties or as diiminopyridine moieties, allows for the coordination of NiBr₂ to the scaffold of the porous polymers. Electronic effects of coordination seem to be stronger in case of the

IL-PON. This fact together with the sheet like morphology of this material render catalysts with a higher concentration of Ni and activities, per atom of Ni, higher than those found for the CTF based materials. Textural properties of the support have been shown to play a key role in product distribution, with meso-CTF and IL-PON displaying a higher selectivity to long chain olefins and a larger degree of deactivation due to the accumulation of long olefins on the catalyst under reaction conditions. Full activity of the mesoporous catalysts can be recovered upon thorough washing with dichlorobenzene.

Our results demonstrate that porous aromatic frameworks hold great promise as catalyst supports: the outstanding stability and rich design tunability of these materials, along with the possibility of including additional heteroatoms for the coordination of metals and their intrinsic hydrophobic nature render PAFs as ideal supports for the heterogenization of molecular complexes.

References

- [1] A. Finiels, F. Fajula, V. Hulea, Nickel-based solid catalysts for ethylene oligomerization - a review, *Catalysis Science & Technology*, 4 (2014) 2412-2426.
- [2] G.R. Lappin, L.H. Nemeč, J.D. Sauer, J.D. Wagner, Olefins, Higher, in: *Kirk-Othmer Encyclopedia of Chemical Technology*, John Wiley & Sons, Inc., 2000.
- [3] C.M. Killian, L.K. Johnson, M. Brookhart, Preparation of Linear α -Olefins Using Cationic Nickel(II) α -Diimine Catalysts, *Organometallics*, 16 (1997) 2005-2007.
- [4] B.L. Small, M. Brookhart, Iron-Based Catalysts with Exceptionally High Activities and Selectivities for Oligomerization of Ethylene to Linear α -Olefins, *Journal of the American Chemical Society*, 120 (1998) 7143-7144.
- [5] S.A. Svejda, M. Brookhart, Ethylene Oligomerization and Propylene Dimerization Using Cationic (α -Diimine)nickel(II) Catalysts, *Organometallics*, 18 (1999) 65-74.
- [6] C. Carlini, M. Marchionna, A.M. Raspolli Galletti, G. Sbrana, Novel α -nitroketonate nickel(II) complexes as homogeneous catalysts for ethylene oligomerization, *Applied Catalysis A: General*, 206 (2001) 1-12.
- [7] W. Keim, R.P. Schulz, Chelate control in the nickel-complex catalysed homogeneous oligomerization of ethylene, *Journal of Molecular Catalysis*, 92 (1994) 21-33.
- [8] A. Boudier, P.-A.R. Breuil, L. Magna, H. Olivier-Bourbigou, P. Braunstein, Nickel(II) complexes with imino-imidazole chelating ligands bearing pendant donor groups (SR, OR, NR₂, PR₂) as precatalysts in ethylene oligomerization, *Journal of Organometallic Chemistry*, 718 (2012) 31-37.
- [9] A.H.D.P.S. Ulbrich, R.R. Campedelli, J.L.S. Milani, J.H.Z.d. Santos, O.d.L. Casagrande Jr, Nickel catalysts based on phenyl ether-pyrazol ligands: Synthesis, XPS study, and use in ethylene oligomerization, *Applied Catalysis A: General*, 453 (2013) 280-286.
- [10] C. Obuah, B. Omondi, K. Nozaki, J. Darkwa, Solvent and co-catalyst dependent pyrazolylpyridinamine and pyrazolylpyrroleamine nickel(II) catalyzed oligomerization and polymerization of ethylene, *Journal of Molecular Catalysis A: Chemical*, 382 (2014) 31-40.
- [11] L. Wang, W.-H. Sun, L. Han, Z. Li, Y. Hu, C. He, C. Yan, Cobalt and nickel complexes bearing 2,6-bis(imino)phenoxy ligands: syntheses, structures and oligomerization studies, *Journal of Organometallic Chemistry*, 650 (2002) 59-64.
- [12] C. Bianchini, G. Giambastiani, L. Luconi, A. Meli, Olefin oligomerization, homopolymerization and copolymerization by late transition metals supported by (imino)pyridine ligands, *Coordination Chemistry Reviews*, 254 (2010) 431-455.

- [13] C. Bianchini, G. Giambastiani, I.G. Rios, G. Mantovani, A. Meli, A.M. Segarra, Ethylene oligomerization, homopolymerization and copolymerization by iron and cobalt catalysts with 2,6-(bis-organylimino)pyridyl ligands, *Coordination Chemistry Reviews*, 250 (2006) 1391-1418.
- [14] W. Zhang, W.-H. Sun, C. Redshaw, Tailoring iron complexes for ethylene oligomerization and/or polymerization, *Dalton Transactions*, 42 (2013) 8988-8997.
- [15] T. Yashima, Y. Ushida, M. Ebisawa, N. Hara, Polymerization of ethylene over transition-metal exchanged Y zeolites, *Journal of Catalysis*, 36 (1975) 320-326.
- [16] F.T.T. Ng, D.C. Creaser, Ethylene dimerization over modified nickel exchanged Y-zeolite, *Applied Catalysis A: General*, 119 (1994) 327-339.
- [17] M. Lallemand, A. Finiels, F. Fajula, V. Hulea, Catalytic oligomerization of ethylene over Ni-containing dealuminated Y zeolites, *Applied Catalysis A: General*, 301 (2006) 196-201.
- [18] D. Barthomeuf, R. Beaumont, X, Y, aluminum-deficient, and ultrastable faujasite-type zeolites: III. Catalytic activity, *Journal of Catalysis*, 30 (1973) 288-297.
- [19] L. Bonneviot, D. Olivier, M. Che, Dimerization of olefins with nickel-surface complexes in X-type zeolite or on silica, *Journal of Molecular Catalysis*, 21 (1983) 415-430.
- [20] I.V. Elev, B.N. Shelimov, V.B. Kazansky, The Role of Ni⁺ Ions in the activity of NiCaY Zeolite catalysts for Ethylene Dimerization, *Journal of Catalysis*, 89 (1984) 470-477.
- [21] F.T.T. Ng, D.C. Creaser, Ethylene Dimerization: Kinetics and Selectivity for 1-Butene, in: J.S. Kevin, C.S. Emerson (Eds.) *Studies in Surface Science and Catalysis*, Elsevier, 1992, pp. 123-131.
- [22] J.R. Sohn, J.H. Park, Characterization of dealuminated NiY zeolite and effect of dealumination on catalytic activity for ethylene dimerization, *Applied Catalysis A: General*, 218 (2001) 229-234.
- [23] A. Martínez, M.A. Arribas, P. Concepción, S. Moussa, New bifunctional Ni-H-Beta catalysts for the heterogeneous oligomerization of ethylene, *Applied Catalysis A: General*, 467 (2013) 509-518.
- [24] J. Heveling, A. van der Beek, M. de Pender, Oligomerization of ethene over nickel-exchanged zeolite γ into a diesel-range product, *Applied Catalysis*, 42 (1988) 325-336.
- [25] M. Lallemand, O.A. Rusu, E. Dumitriu, A. Finiels, F. Fajula, V. Hulea, Ni-MCM-36 and Ni-MCM-22 catalysts for the ethylene oligomerization, in: P.M. Antoine Gédéon, B. Florence (Eds.) *Studies in Surface Science and Catalysis*, Elsevier, 2008, pp. 1139-1142.
- [26] M. Lallemand, O.A. Rusu, E. Dumitriu, A. Finiels, F. Fajula, V. Hulea, NiMCM-36 and NiMCM-22 catalysts for the ethylene oligomerization: Effect of zeolite texture and nickel cations/acid sites ratio, *Applied Catalysis A: General*, 338 (2008) 37-43.
- [27] V. Hulea, F. Fajula, Ni-exchanged AlMCM-41—An efficient bifunctional catalyst for ethylene oligomerization, *Journal of Catalysis*, 225 (2004) 213-222.
- [28] M. Lallemand, A. Finiels, F. Fajula, V. Hulea, Continuous stirred tank reactor for ethylene oligomerization catalyzed by NiMCM-41, *Chemical Engineering Journal*, 172 (2011) 1078-1082.
- [29] M. Hartmann, A. Pöppel, L. Kevan, Ethylene dimerization in nickel containing MCM-41 and AlMCM-41 studied by electron spin resonance and gas chromatography, in: W.N.D.E.I. Joe W. Hightower, T.B. Alexis (Eds.) *Studies in Surface Science and Catalysis*, Elsevier, 1996, pp. 801-809.
- [30] M. Lallemand, A. Finiels, F. Fajula, V. Hulea, Ethylene oligomerization over Ni-containing mesostructured catalysts with MCM-41, MCM-48 and SBA-15 topologies, in: Z.G.J.C. Ruren Xu, Y. Wenfu (Eds.) *Studies in Surface Science and Catalysis*, Elsevier, 2007, pp. 1863-1869.
- [31] M.O. de Souza, L.R. Rodrigues, H.O. Pastore, J.A.C. Ruiz, L. Gengembre, R.M. Gauvin, R.F. de Souza, A nano-organized ethylene oligomerization catalyst: Characterization and reactivity of the Ni(MeCN)₆(BF₄)₂/[Al]-MCM-41/AlEt₃ system, *Microporous and Mesoporous Materials*, 96 (2006) 109-114.
- [32] A. Lacarriere, J. Robin, D. Świerczyński, A. Finiels, F. Fajula, F. Luck, V. Hulea, Distillate-Range Products from Non-Oil-Based Sources by Catalytic Cascade Reactions, *ChemSusChem*, 5 (2012) 1787-1792.
- [33] S. Lin, L. Shi, H. Zhang, N. Zhang, X. Yi, A. Zheng, X. Li, Tuning the pore structure of plug-containing Al-SBA-15 by post-treatment and its selectivity for C₁₆ olefin in ethylene oligomerization, *Microporous and Mesoporous Materials*, 184 (2014) 151-161.
- [34] T. Cai, D. Cao, Z. Song, L. Li, Catalytic behavior of NiSO₄/ γ -Al₂O₃ for ethene dimerization, *Applied Catalysis A: General*, 95 (1993) L1-L7.
- [35] T. Cai, Studies of a new alkene oligomerization catalyst derived from nickel sulfate, *Catalysis Today*, 51 (1999) 153-160.
- [36] J.R. Sohn, W.C. Park, Nickel sulfate supported on γ -Al₂O₃ for ethylene dimerization, *Journal of Molecular Catalysis A: Chemical*, 133 (1998) 297-301.
- [37] J.R. Sohn, W.C. Park, H.W. Kim, Characterization of Nickel Sulfate Supported on γ -Al₂O₃ for Ethylene Dimerization and Its Relationship to Acidic Properties, *Journal of Catalysis*, 209 (2002) 69-74.
- [38] J.R. Sohn, W.C. Park, The roles of active sites of nickel sulfate supported on γ -Al₂O₃ for ethylene dimerization, *Applied Catalysis A: General*, 239 (2003) 269-278.
- [39] J.R. Sohn, E.S. Cho, Promoting effect of Al₂O₃ on catalytic activity of NiSO₄/ZrO₂ for ethylene dimerization, *Applied Catalysis A: General*, 282 (2005) 147-154.
- [40] W. Hua, Y. Xia, Y. Yue, Z. Gao, Promoting Effect of Al on SO₂-4/MxO_y (M=Zr, Ti, Fe) Catalysts, *Journal of Catalysis*, 196 (2000) 104-114.
- [41] J.R. Sohn, S.H. Lee, Effect of TiO₂-ZrO₂ composition on catalytic activity of supported NiSO₄ for ethylene dimerization, *Applied Catalysis A: General*, 321 (2007) 27-34.

- [42] J.P. Hogan, R.L. Banks, W.C. Lanning, A. Clark, Polymerization of Light Olefins over Nickel Oxide–Silica–Alumina, *Industrial & Engineering Chemistry*, 47 (1955) 752-757.
- [43] A.V. Lavrenov, E.A. Bulucheuskii, M.A. Moiseenko, V.A. Drozdov, A.B. Arbuzov, T.I. Gulyaeva, V.A. Likholobov, V.K. Duplyakin, Chemical composition optimization and characterization of the NiO/B₂O₃-Al₂O₃ system as a catalyst for ethylene oligomerization, *Kinetics and Catalysis*, 51 (2010) 404-409.
- [44] J.R. Sohn, D.C. Shin, New Catalyst of NiO–ZrO₂/WO₃ for Ethylene Dimerization, *Journal of Catalysis*, 160 (1996) 314-316.
- [45] J.R. Sohn, S.H. Kwon, D.C. Shin, Spectroscopic studies on NiO supported on ZrO₂ modified with MoO₃ for ethylene dimerization, *Applied Catalysis A: General*, 317 (2007) 216-225.
- [46] J.R. Sohn, S.Y. Lee, High catalytic activity of NiO/ZrO₂ modified with WO₃ for ethylene dimerization, *Applied Catalysis A: General*, 164 (1997) 127-140.
- [47] J.R. Sohn, H.J. Kim, High catalytic activity of NiO • TiO₂SO₂– for ethylene dimerization, *Journal of Catalysis*, 101 (1986) 428-433.
- [48] J.R. Sohn, H.W. Kim, M.Y. Park, E.H. Park, J.T. Kim, S.E. Park, Highly active catalyst of NiO–ZrO₂ modified with H₂SO₄ for ethylene dimerization, *Applied Catalysis A: General*, 128 (1995) 127-141.
- [49] J. Heveling, C.P. Nicolaides, M.S. Scurrall, Catalysts and conditions for the highly efficient, selective and stable heterogeneous oligomerization of ethylene, *Applied Catalysis A: General*, 173 (1998) 1-9.
- [50] J. Heveling, C.P. Nicolaides, Chain-Length Distributions Obtained over Nickel(II)-Exchanged or Impregnated Silica–Alumina Catalysts for the Oligomerization of Lower Alkenes, *Catalysis Letters*, 107 (2006) 117-121.
- [51] R.L. Espinoza, R. Snel, C.J. Korf, C.P. Nicolaides, Catalytic oligomerization of ethene over nickel-exchanged amorphous silica-aluminas; effect of the acid strength of the support, *Applied Catalysis*, 29 (1987) 295-303.
- [52] R.L. Espinoza, C.P. Nicolaides, C.J. Korf, R. Snel, Catalytic oligomerization of ethene over nickel-exchanged amorphous silica-alumina; Effect of the nickel concentration, *Applied Catalysis*, 31 (1987) 259-266.
- [53] M.D. Heydenrych, C.P. Nicolaides, M.S. Scurrall, Oligomerization of Ethene In a Slurry Reactor Using a Nickel(II)-Exchanged Silica–Alumina Catalyst, *Journal of Catalysis*, 197 (2001) 49-57.
- [54] Z. Ye, H. Alsyouri, S. Zhu, Y.S. Lin, Catalyst impregnation and ethylene polymerization with mesoporous particle supported nickel-diimine catalyst, *Polymer*, 44 (2003) 969-980.
- [55] E. Rossetto, M. Caovilla, D. Thiele, R.F. de Souza, K. Bernardo-Gusmão, Ethylene oligomerization using nickel-β-diimine hybrid xerogels produced by the sol–gel process, *Applied Catalysis A: General*, 454 (2013) 152-159.
- [56] S.M. Alshehri, T. Ahmad, A. Aldalbahi, N. Alhokbany, Pyridylimine Cobalt(II) and Nickel(II) Complex Functionalized Multiwalled Carbon Nanotubes and Their Catalytic Activities for Ethylene Oligomerization, *Advances in Polymer Technology*, 35 (2016) n/a-n/a.
- [57] L. Zhang, E. Castillejos, P. Serp, W.-H. Sun, J. Durand, Enhanced ethylene polymerization of Ni(II) complexes supported on carbon nanotubes, *Catalysis Today*, 235 (2014) 33-40.
- [58] H. Kurokawa, M. Matsuda, K. Fujii, Y. Ishihama, T. Sakuragi, M.-a. Ohshima, H. Miura, Bis(imino)pyridine Iron and Cobalt Complexes Immobilized into Interlayer Space of Fluorotetrasilicic Mica: Highly Active Heterogeneous Catalysts for Polymerization of Ethylene, *Chemistry Letters*, 36 (2007) 1004-1005.
- [59] K. Fujii, Y. Ishihama, T. Sakuragi, M.-a. Ohshima, H. Kurokawa, H. Miura, Heterogeneous catalysts immobilizing α-diimine nickel complexes into fluorotetrasilicic mica interlayers to prepare branched polyethylene from only ethylene, *Catalysis Communications*, 10 (2008) 183-186.
- [60] T. Kondo, K. Yamamoto, T. Sakuragi, H. Kurokawa, H. Miura, Acetylaminopyridineiron(III) Complexes Immobilized in Fluorotetrasilicic Mica Interlayer as Efficient Catalysts for Oligomerization of Ethylene, *Chemistry Letters*, 41 (2012) 461-463.
- [61] H. Kurokawa, K. Miura, K. Yamamoto, T. Sakuragi, T. Sugiyama, M.-a. Ohshima, H. Miura, Oligomerization of Ethylene to Produce Linear α-Olefins Using Heterogeneous Catalyst Prepared by Immobilization of α-Diiminonickel(II) Complex into Fluorotetrasilicic Mica Interlayer, *Catalysts*, 3 (2013) 125.
- [62] H. Kurokawa, M. Hayasaka, K. Yamamoto, T. Sakuragi, M.-a. Ohshima, H. Miura, Self-assembled heterogeneous late transition–metal catalysts for ethylene polymerization; New approach to simple preparation of iron and nickel complexes immobilized in clay mineral interlayer, *Catalysis Communications*, 47 (2014) 13-17.
- [63] R. Malgas-Enus, S.F. Mapolie, Nickel metallo dendrimers as catalyst precursors in the tandem oligomerization of ethylene and Friedel–Crafts alkylation of its olefinic products, *Inorganica Chimica Acta*, 409, Part A (2014) 96-105.
- [64] K. Kyogoku, C. Yamada, Y. Suzuki, S. Nishiyama, K. Fukumoto, H. Yamamoto, S. Indo, M. Sano, T. Miyake, Syntheses of Metal-organic Framework Compounds Containing Ni-bipyridyl Complex for Oligomerization of Ethylene, *Journal of the Japan Petroleum Institute*, 53 (2010) 308-312.
- [65] J. Canivet, S. Aguado, Y. Schuurman, D. Farrusseng, MOF-Supported Selective Ethylene Dimerization Single-Site Catalysts through One-Pot Postsynthetic Modification, *Journal of the American Chemical Society*, 135 (2013) 4195-4198.
- [66] B. Liu, S. Jie, Z. Bu, B.-G. Li, Postsynthetic modification of mixed-linker metal-organic frameworks for ethylene oligomerization, *RSC Advances*, 4 (2014) 62343-62346.
- [67] S. Liu, Y. Zhang, Q. Huo, S. He, Y. Han, Synthesis and catalytic performances of a novel Zn-MOF catalyst bearing nickel chelating diimine carboxylate ligands for ethylene oligomerization, *Journal of Spectroscopy*, 2015 (2015).
- [68] S.T. Madrahimov, J.R. Gallagher, G. Zhang, Z. Meinhardt, S.J. Garibay, M. Delferro, J.T. Miller, O.K. Farha, J.T. Hupp, S.T. Nguyen, Gas-Phase Dimerization of Ethylene under Mild Conditions Catalyzed by MOF Materials Containing (bpy)Ni(II) Complexes, *ACS Catalysis*, 5 (2015) 6713-6718.

- [69] E.D. Metzger, C.K. Brozek, R.J. Comito, M. Dincă, Selective Dimerization of Ethylene to 1-Butene with a Porous Catalyst, *ACS Central Science*, 2 (2016) 148-153.
- [70] F. Speiser, P. Braunstein, L. Saussine, Catalytic Ethylene Dimerization and Oligomerization: Recent Developments with Nickel Complexes Containing P,N-Chelating Ligands, *Accounts of Chemical Research*, 38 (2005) 784-793.
- [71] Z. Boudene, A. Boudier, P.-A.R. Breuil, H. Olivier-Bourbigou, P. Raybaud, H. Toulhoat, T. de Bruin, Understanding the role of aluminum-based activators in single site iron catalysts for ethylene oligomerization, *Journal of Catalysis*, 317 (2014) 153-157.
- [72] A. de la Peña Ruigómez, D. Rodríguez-San-Miguel, K.C. Stylianou, M. Cavallini, D. Gentili, F. Liscio, S. Milita, O.M. Roscioni, M.L. Ruiz-González, C. Carbonell, D. Maspoch, R. Mas-Ballesté, J.L. Segura, F. Zamora, Direct On-Surface Patterning of a Crystalline Laminar Covalent Organic Framework Synthesized at Room Temperature, *Chemistry – A European Journal*, 21 (2015) 10666-10670.
- [73] A.V. Bavykina, M.G. Goesten, F. Kapteijn, M. Makkee, J. Gascon, Efficient production of hydrogen from formic acid using a Covalent Triazine Framework supported molecular catalyst, *ChemSusChem*, 8 (2015) 809-812.
- [74] F.J. Uribe-Romo, J.R. Hunt, H. Furukawa, C. Klöck, M. O’Keeffe, O.M. Yaghi, A Crystalline Imine-Linked 3-D Porous Covalent Organic Framework, *Journal of the American Chemical Society*, 131 (2009) 4570-4571.
- [75] T. Rodenas, I. Luz, G. Prieto, B. Seoane, H. Miro, A. Corma, F. Kapteijn, F.X. Llabrés i Xamena, J. Gascon, Metal-organic framework nanosheets in polymer composite materials for gas separation, *Nat Mater*, 14 (2015) 48-55.
- [76] A.V. Bavykina, E. Rozhko, M.G. Goesten, T. Wezendonk, B. Seoane, F. Kapteijn, M. Makkee, J. Gascon, Shaping Covalent Triazine Frameworks for the Hydrogenation of Carbon Dioxide to Formic Acid, *ChemCatChem*, 8 (2016) 2217-2221.
- [77] J. Matienzo, L.I. Yin, S.O. Grim, W.E. Swartz, X-ray photoelectron spectroscopy of nickel compounds, *Inorganic Chemistry*, 12 (1973) 2762-2769.
- [78] K. Artyushkova, B. Kiefer, B. Halevi, A. Knop-Gericke, R. Schlogl, P. Atanassov, Density functional theory calculations of XPS binding energy shift for nitrogen-containing graphene-like structures, *Chemical Communications*, 49 (2013) 2539-2541.
- [79] M. Soorholtz, L.C. Jones, D. Samuelis, C. Weidenthaler, R.J. White, M.-M. Titirici, D.A. Cullen, T. Zimmermann, M. Antonietti, J. Maier, R. Palkovits, B.F. Chmelka, F. Schüth, Local Platinum Environments in a Solid Analogue of the Molecular Periana Catalyst, *ACS Catalysis*, 6 (2016) 2332-2340.
- [80] G.A. Nesterov, V.A. Zakharov, G. Fink, W. Fenzl, Supported nickel catalysts for ethylene oligomerization, *Journal of Molecular Catalysis*, 69 (1991) 129-136.
- [81] E. Angelescu, M. Che, M. Andruh, R. Zăvoianu, G. Costentin, C. Mirică, O. Dumitru Pavel, Ethylene selective dimerization on polymer complex catalyst of Ni(4,4'-bipyridine)Cl₂ coactivated with AlCl(C₂H₅)₂, *Journal of Molecular Catalysis A: Chemical*, 219 (2004) 13-19.
- [82] D. Schaarschmidt, J. Kühnert, S. Tripke, H.G. Alt, C. Görl, T. Ruffer, P. Ecorchard, B. Walfort, H. Lang, Ferrocenyl phosphane nickel carbonyls: Synthesis, solid state structure, and their use as catalysts in the oligomerization of ethylene, *Journal of Organometallic Chemistry*, 695 (2010) 1541-1549.
- [83] R. Gao, M. Zhang, T. Liang, F. Wang, W.-H. Sun, Nickel(II) Complexes Chelated by 2-Arylimino-6-benzoxazolylpyridine: Syntheses, Characterization, and Ethylene Oligomerization, *Organometallics*, 27 (2008) 5641-5648.